# Prediction of ferroelectric stability and magnetoelectric effect of asymmetric multiferroic tunnel junctions

X. T. Liu, Yue Zheng' , B. Wang' , and W. J. Chen

Citation: Appl. Phys. Lett. **102**, 152906 (2013); doi: 10.1063/1.4801306
View online: http://dx.doi.org/10.1063/1.4801306
View Table of Contents: http://aip.scitation.org/toc/apl/102/15
Published by the American Institute of Physics

# Prediction of ferroelectric stability and magnetoelectric effect of asymmetric multiferroic tunnel junctions

X. T. Liu,[1,2] Yue Zheng,[1,2,a)] B. Wang,[1,2,b)] and W. J. Chen[1,2]
[1]*State Key Laboratory of Optoelectronic Materials and Technologies, School of Physics and Engineering, Sun Yat-sen University, 510275 Guangzhou, China*
[2]*Micro&Nano Physics and Mechanics Research Laboratory, School of Physics and Engineering, Sun Yat-sen University, 510275 Guangzhou, China*

(Received 31 January 2013; accepted 21 March 2013; published online 17 April 2013)

Taking into account size effect of the ferroelectric tunnel barrier and interface effect determined by two dissimilar magnetic electrodes, the ferroelectric stability and magnetoelectric effect of asymmetric multiferroic tunnel junctions have been comprehensively calculated. Results of the stable structure, polarization, electrostatic potential, charge density, spin density, and magnetic moments demonstrated a series of the great hidden features in asymmetric multiferroic tunnel junctions and showed significant differences between two polarization states. The potential and magnetic moment are strongly affected by electric and magnetic polarizations, suggesting the possibility of ferroelectric control of magnetization and coexistence of tunnel magnetoresistance and giant electroresistance effects. © *2013 American Institute of Physics*. [http://dx.doi.org/10.1063/1.4801306]

Multiferroic tunnel junctions (MFTJs) have attracted much scientific interests for their possible applications in multifunctional electronic devices.[1–12] As a combination of magnetic tunnel junctions (MTJs) and ferroelectric tunnel junctions (FTJs), MFTJs inherit novel electronic properties originally existing severally in MTJs and FTJs, including tunneling magnetoresistance,[8,9] giant electroresistance,[6,7] giant piezoelectric resistance,[11,12] and non-destructive read out effects.[2] In addition, the interaction between ferromagnetism and ferroelectricity in MFTJs gives rise to magnetoelectric effect,[3,5,13–18] allowing magnetic (electric) controls of ferroelectric (magnetic) properties. The control and utilization of the charge and spin degrees of freedom in spintronic devices has been an attractive issue in recent years, and tremendous endeavors were made to explore the mechanism of controlling the magnetic and electric properties in MTFJs.

It has been realized that magnetoelectric properties of the nanoscale MFTJs can be significantly affected by many factors, such as thickness, misfit strain, surface, and interface.[1,7,12,13] Particularly, the size effect of MFTJs posts a difficulty in developing nanoscale spintronic devices based on MFTJ units, for the reason that it is intractable to have remarkable ferroelectricity to affect the transport in an extremely small scale.[14–21] It is well known that the spontaneous polarization disappears as the thickness of a ferroelectric barrier is below a critical thickness,[22–26] while electrons can tunnel through a insulating barrier of only a few nanometers and will damp exponentially as the thickness increases. Various means have been worked out to maintain ferroelectricity as well as conductivity in ferroelectric tunnel junctions, such as imposing misfit strain by lattice mismatch,[22] improving screening of electrodes,[24] and employing appropriate compound materials to make use of the interface effect. A typical MFTJ consists of two metal electrodes separated by a ferroelectric/multiferroic thin film as a barrier where at least two of the three components have switchable magnetization. For example, a MFTJ with a multiferroic $La_{0.1}Bi_{0.9}MnO_3$ barrier sandwiched by a magnetic electrode and a nonmagnetic electrode has been reported to show four resistance states.[17] Considering the scarcity of single phase multiferroic materials,[20] a promising alternative is the heterojunction with two magnetic electrodes and a ferroelectric barrier.[10,21] Moreover, exploiting dissimilar magnetic electrodes can further introduce an asymmetry and cause a built-in field, which can be originated from various sources such as work functions difference, the dipolar imhomogenesities,[27–30] and mismatch effect.[29] The built-in field has been predicted to show various influence on the phase transition in ferroelectric thin films such as smearing the phase transition[28,30] and eliminating non-polar paraelectric phase.[27]

In this paper, we perform first-principle simulations to investigate the Fe/$BaTiO_3$/Co MFTJs. We demonstrate how the ferroelectric stability is affected by the asymmetric interfaces introduced by polarization and dissimilar electrodes, and how the magnetic properties at the ferroelectric-electrode interfaces are coupled with ferroelectric polarization switching. Our simulations also suggest the possibility of ferroelectric control of magnetization and coexistence of tunnel magnetoresistance and giant electroresistance effects in MFTJs.

All calculations are performed within the spin-polarized density-functional theory (DFT) as implemented in Vienna *ab initio* Simulation Package[31,32] (VASP) using the projector augmented wave (PAW) method. The exchange-correlation potential is treated in the local density approximation (LDA). The plane wave functions are expanded with the energy cutoff of 500 eV. All the atoms are relaxed using a $6 \times 6 \times 1$ Monkhorst Pack grid for $k$-point sampling until the Hellmann-Feynman force on each atom is less than 10 meV/Å. The MFTJ under the short-circuit boundary condition is created by constructing a superlattice under periodic boundary conditions.[33] The Fe/$BaTiO_3$/Co layers are stacked along the [001] direction ($z$ direction) of the bulk $BaTiO_3$ with $BaTiO_3$ layers

a)Author to whom correspondence should be addressed. Electronic mail: zhengy35@mail.sysu.edu.cn
b)Electronic mail: wangbiao@mail.sysu.edu.cn

 

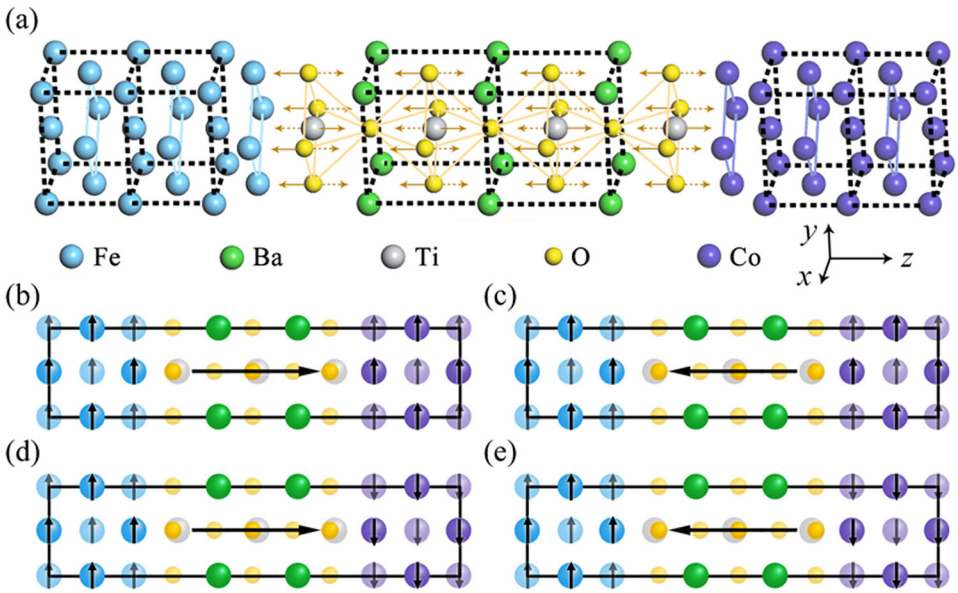


FIG. 1. (a) Atomic structures of Fe/$BaTiO_3$/Co MFTJ. (b)–(e) Schematics of the four magnetoelectric states of P→M↑↑, P←M↑↑, P→M↑↓, and P←M↑↓, respectively. The lighter color of atoms indicates deeper positions.

terminated by $TiO_2$, as depicted in Figure 1 and Figure S1. For convenience, in the following, P→ corresponds to the polarization pointing from Fe/$BaTiO_3$ interface to Co/$BaTiO_3$ interface, and P← is the opposite. Similarly, M↑↑ and M↑↓ denote parallel and antiparallel magnetization of the two electrodes, respectively. The in-plane lattice constant of the supercell is constrained to the bulk lattice constant of $SrTiO_3$, i.e., 3.866 Å, to simulate a junction grown on $SrTiO_3$ substrate. The distances between the $BaTiO_3$ layers and the electrodes at the equilibrium conditions are obtained by minimizing the total energy of the entire heterostructure, which are determined to be 1.57 Å and 1.70 Å for the Fe/$BaTiO_3$ interface and the Co/$BaTiO_3$ interface, respectively. $BaTiO_3$ layers with different thicknesses are employed to study the impact of barrier thickness on properties of the MFTJs. The Fe electrode and Co electrode are fixed to be 9 monolayers of atoms and 8 monolayers of atoms, respectively. Thus, the supercell is constructed as $Fe_{18}/TiO_2$-$(BaO\text{-}TiO_2)_m/Co_{16}$, where $m = 2$, 3, 4, 5, 6, 8, 10. To obtain the ferroelectric displacements, we impose an initial displacement of Ti atoms along [001] direction with respect to the O atoms in the same *x*-*y* plane and then fully relax all of the atoms in the supercell.

To investigate the ferroelectric instability, Figure 2 presents the layer-resolved relative Ti-O displacements in the $BaTiO_3$ multilayer for different $BaTiO_3$ film thicknesses. As the film thickness increases, it can be seen that the Ti-O displacements become larger and gradually approach the bulk value 0.167 Å. The Ti-O displacements are smaller near the interfaces, implying a depressing effect of interface on the ferroelectricity of $BaTiO_3$ film. In contrast to the results of FTJs with symmetric electrodes,[15,22] our result shows that the critical thickness of ferroelectricity vanishes in Fe/$BaTiO_3$/Co system. Particularly, the displacements throughout the entire $BaTiO_3$ film are of the same sign even for the $BaTiO_3$ layer containing only two unit cells ($m = 2$). When the $BaTiO_3$ film is less than four unit cells, the Ti-O relative displacements are all negative for either positive or negative initial Ti-O displacements. Thus, it shows that the P→ state is unstable and will spontaneously reverse to the P← state. Comparing Figures 2(a) and 2(b), the difference caused by magnetization configuration of the electrodes is negligible.

Using the Berry phase method,[34,35] the polarization $P$ of MFTJ is evaluated according to the formula $P = \frac{e}{\Omega}\sum_i Z_i^* u_i$, where $Z_i^*$ is the Born effective charge and $u_i$ is the

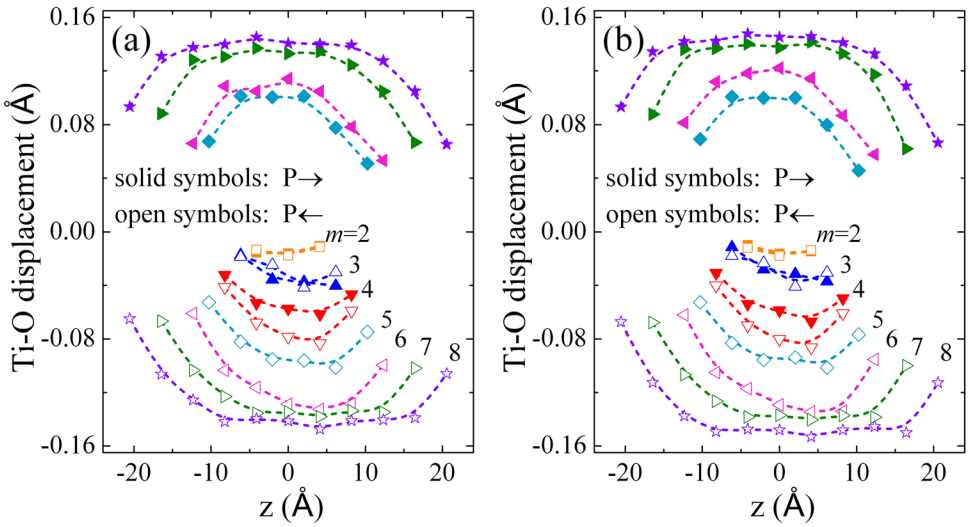


FIG. 2. The relative Ti-O displacement along the *z*-axis direction of the supercell for different thicknesses of $BaTiO_3$ films with the magnetization of electrodes being parallel (a) and anti-parallel (b). The legend indicates the initial states.

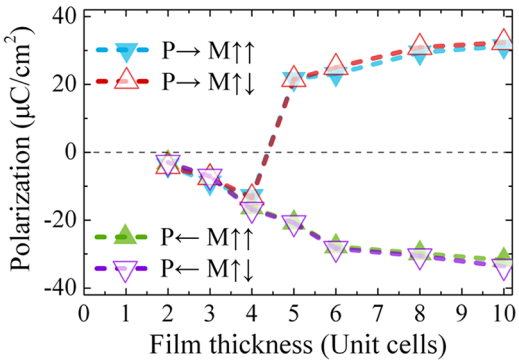


FIG. 3. Equilibrium average polarization as a function of $BaTiO_3$ thin film thickness for four magnetoelectric states. Note that the legend corresponds only to the initial configuration.

displacement of the ion $i$ in the ferroelectric state with respect to the paraelectric state. The calculated Born effective charges are 2.71 and 6.62 for Ba and Ti, respectively, and −5.02 and −2.08 for O in the BaO and $TiO_2$ planes, respectively. As shown in Figure 3, the average polarization of the $BaTiO_3$ thin film is nonzero for all thicknesses and approaches to bulk value as the thickness increases. It is interesting to note that, consistent with the result derived from Figure 2, for $BaTiO_3$ films with $m \leq 4$, the average polarization necessarily points from Co electrode to Fe electrode in spite of the signs of initial relative Ti-O displacements, indicating the polarization bistability vanished.

To clarify the mechanism of the vanishing of the polarization bistability, we further calculate the macroscopic electrostatic potential energy of the junction. Figure 4 shows the results for four initial magnetoelectric states for $m = 3, 4, 5, 6$, respectively. All the subfigures show a discrepancy in the Co electrode area for two magnetic states. Although switching the magnetization configuration leads to distinct changing of the electrostatic potential of the electrodes, it makes negligible difference in the barrier region. For $m = 3$ and $m = 4$, the potential profiles across the ferroelectric barrier are almost the same with higher potential on the right side of the barrier. For $m = 5$ and $m = 6$, reversing the initial polarization results in an opposite tendency of the potential profile across the barrier, which indicates that the polarization of ferroelectric film becomes bistable in the system. More importantly, for $m = 5$ and $m = 6$, a slight but discernible difference can be found in the absolute of the slope of the potential profiles, indicating the existence of a built-in field. For $m = 5$, by linearly fitting the potential energy within the ferroelectric barrier, we obtain the total electric field to be $-3.8 \times 10^8$ V/cm and $2.7 \times 10^8$ V/cm corresponding to P→ state and P← state, respectively.

The origin of the built-in field is the introduction of asymmetric interfaces, which leads to quite different screening and bonding environments at the interfaces. To estimate the built-in field, we further calculate the electrostatic potential energy of Fe/$BaTiO_3$/Co systems for $m = 5$ with zero initial Ti-O displacement so as to exclude the influence of the screening field resulting from the polarization. We obtained a built-in field purely produced by the dissimilar electrodes as about $-0.3 \times 10^8$ V/cm, which points from Co/$BaTiO_3$ interface to Fe/$BaTiO_3$ interface. Due to this field, there will be nonzero polarization even the film is only two unit cells thick. As the ferroelectric film becomes thicker, the built-in field decreasing with thickness makes relatively small difference between two polarization directions so that the system becomes bistable. More essentially, the built-in field across the film should be driven by the contact potential difference between the two insulator-electrode interfaces. Therefore, we estimate the built-in field by $\vec{E}_{bi} = (\Delta\phi_2 - \Delta\phi_1)(ed)^{-1}\vec{n}$, where $\Delta\phi_1$ and $\Delta\phi_2$ are the Schottky barrier heights at the Fe/$BaTiO_3$ and Co/$BaTiO_3$ interfaces, respectively, $e$ is the elementary positive charge, $d$ is the thickness of the ferroelectric film, and $\vec{n}$ is the unit normal vector of $x$-$y$ plane. The Schottky barrier is calculated using the method described in a recent work by Umeno *et al.*[36] Because it is difficult to introduce the impact of magnetization configuration into such a model and the magnetization shows indistinctive impact on polarization according to Figure 4, we alternatively performed nonmagnetic calculation for reference. From the

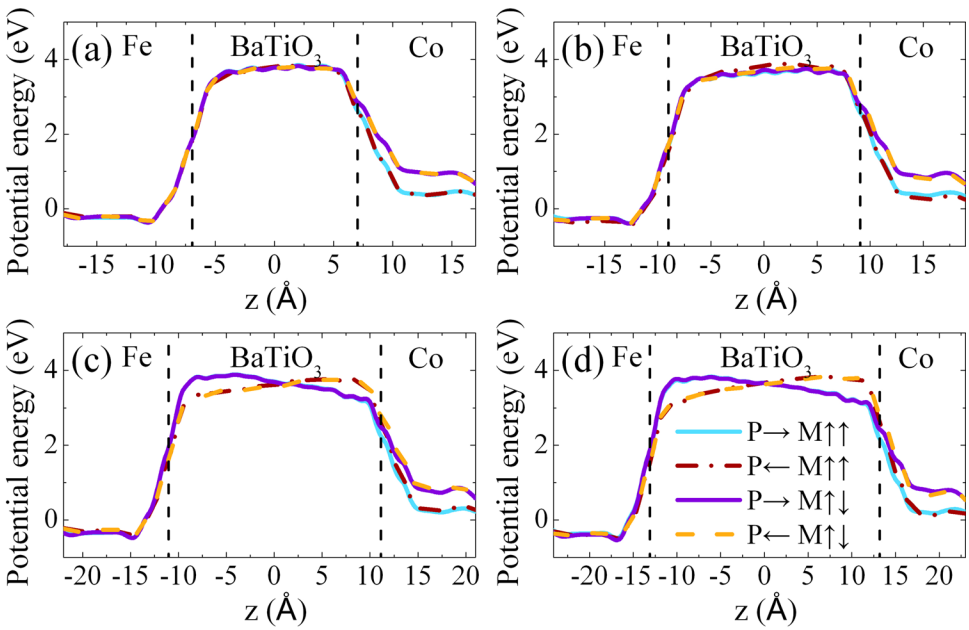


FIG. 4. Profile of macroscopic planar averaged electrostatic potential energy felt by electrons of the junction for four magnetoelectric states for $m = 3, 4, 5, 6$. The interfaces are indicated by vertical dashed lines.

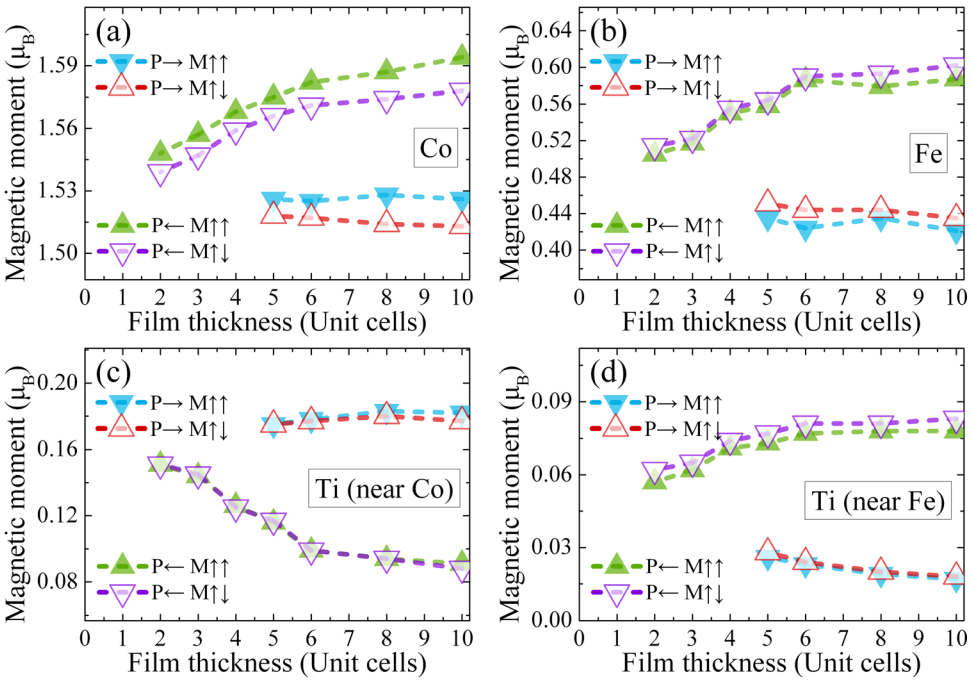


FIG. 5. Absolute values of magnetic moments (in unit of $\mu_B$) of Fe, Co, and Ti atoms at the interfaces for MFTJs with different film thicknesses.

calculated Schottky barrier, the built-in field in a nonmagnetic Fe/$BaTiO_3$/Co tunnel junction is obtained as $-0.5 \times 10^8$ V/cm, which is close to the value calculated from the slope of potential profile and further validates the existence of the built-in field from Co electrode to Fe electrode.

To investigate the magnetic properties of interfaces affected by the orientations of polarizations, we also calculate the magnetic moments of the atoms at interfaces as displayed in Figure 5 and in Table S1 (see supporting information[37]). Ti atoms possess net magnetic moments despite their zero initial spins while magnetic moments of Fe and Co atoms are all less than the bulk value. In addition, the magnetic moments of Ti atoms are all antiparallel to those of their neighbor Fe and Co atoms, indicating charge redistribution between majority and

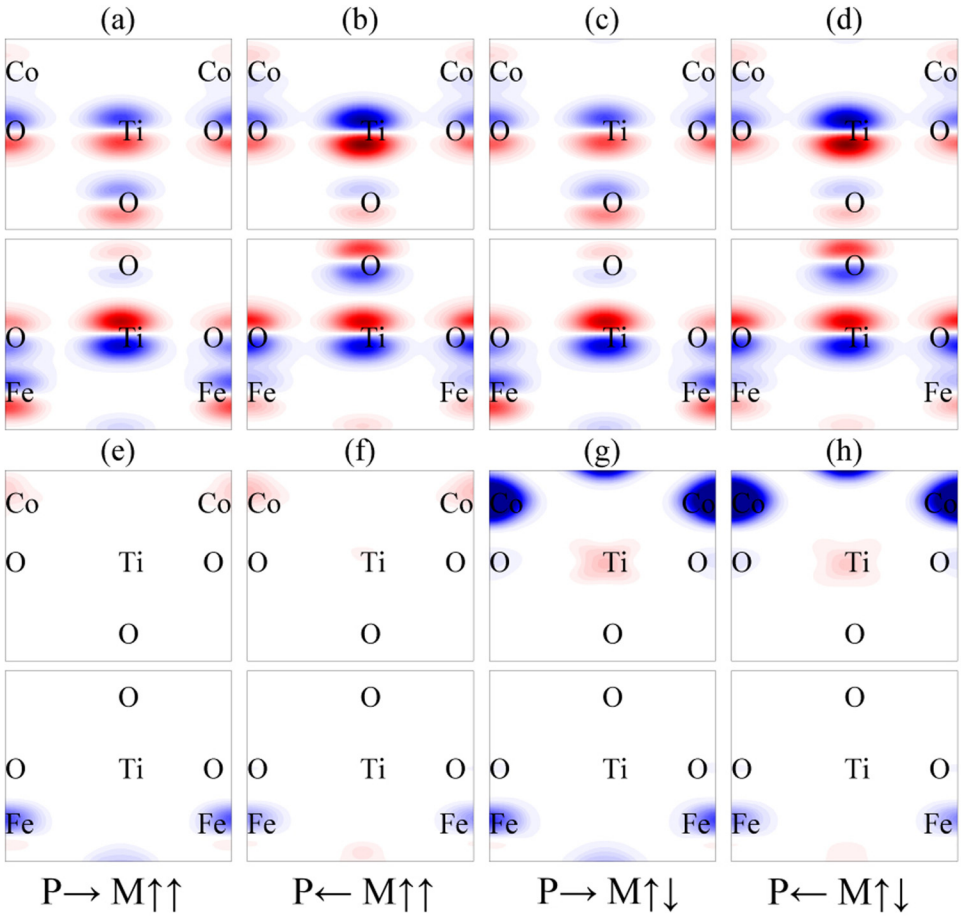


FIG. 6. Differential charge density (a)–(d) and differential spin density (e)–(h) in the *y*-middle plane of Fe/$BaTiO_3$/Co supercell corresponding to four magnetoelectric states, where red refers to positive value and blue refers to negative value.

minority spins at the interfaces.[15] Particularly, as the film is thicker, the induced magnetic moment of Ti atom increases at the interface which the polarization points to, and decreases at the interface which the polarization points away. On the other hand, the magnetic moments of Co atoms are much larger than Fe atoms, causing the induced magnetic moments of Ti atoms near Co atoms larger than those near Fe atoms as well. Figure 6 depicts the differential charge density and differential spin density in the *y*-middle plane of $Fe/BaTiO_3/Co$ supercell corresponding to four magnetoelectric states. From the differential charge density shown in Figure 6, the charge transfer at the interface which the polarization points to is stronger than that at the other interface. This indicates a possibility of controlling tunneling magnetoresistance via modulating electric polarization, as is achieved experimentally in a similar MFTJ in a latest work.[19]

In conclusion, we have investigated the ferroelectric stability and the interplay of magnetic and electric properties in $Fe/BaTiO_3/Co$ asymmetric multiferroic tunnel junction using the first-principle calculating method based on density functional theory. Our results evidence the existence of a built-in electric field resulting from the contact potential difference between the two insulator-electrode interfaces, which leads to the vanishing critical thickness of ferroelectricity of the perovskite ferroelectric barrier and makes the system become bistable only beyond a critical thickness of 5 unit cells. It is revealed that the potential profile is distinctly changed when the ferroelectric polarization of the barrier is reversed and/or when the magnetic configuration of the two electrodes is switched, indicating the possibility of switching four resistance states in such MFTJs. In addition, reversing the ferroelectric polarization also alters the induced magnetic moments on atoms at the interfaces, which predicts that magnetic properties might be controlled by ferroelectricity. We expect that our work can stimulate further studies on MFTJs and contribute to the development of multifunctional spintronic devices.

The authors gratefully acknowledge the financial support of NSFC (Nos. 10902128, 10732100, 50802026, 10972239). Y. Zheng also thanks support by the Fundamental Research Funds for the Central Universities, NCET in University, Research Fund for the Doctoral Program of Higher Education, and Fok Ying Tung Foundation, Science and Technology Innovation Project of Guangdong Provincial Education Department and Guangdong Natural Science Funds for Distinguished Young Scholar.

[1]J. P. Velev, P. A. Dowben, E. Y. Tsymbal, S. J. Jenkins, and A. N. Caruso, Surf. Sci. Rep. **63**, 400 (2008).
[2]V. Garcia, S. Fusil, K. Bouzehouane, S. E. Vedrenne, N. D. Mathur, A. Barthélémy, and M. Bibes, Nature **460**, 81 (2009).
[3]J. P. Velev, C. G. Duan, J. D. Burton, A. Smogunov, M. K. Niranjan, E. Tosatti, S. S. Jaswal, and E. Y. Tsymbal, Nano Lett. **9**, 427 (2009).
[4]J. F. Scott, Nature Mater. **6**, 256 (2007).
[5]F. Yang, M. H. Tang, Z. Ye, Y. C. Zhou, X. J. Zheng, J. X. Tang, and J. J. Zhang, J. Appl. Phys. **102**, 044504 (2007).
[6]M. Y. Zhuravlev, R. F. Sabirianov, S. S. Jaswal, and E. Y. Tsymbal, Phys. Rev. Lett. **94**, 246802 (2005).
[7]E. Y. Tsymbal and H. Kohlstedt, Science **313**, 181 (2006).
[8]J. Mathon and A. Umerski, Phys. Rev. B **63**, 220403 (2001).
[9]S. Ikeda, J. Hayakawa, Y. Ashizawa, Y. M. Lee, K. Miura, H. Hasegawa, M. Tsunoda, F. Matsukura, and H. Ohno, Appl. Phys. Lett. **93**, 082508 (2008).
[10]J. D. Burton and E. Y. Tsymbal, Phys. Rev. Lett. **106**, 157203 (2011).
[11]Y. Zheng and C. H. Woo, Nanotechnology **20**, 075401 (2009).
[12]X. Luo, B. Wang, and Y. Zheng, ACS Nano **5**, 1649 (2011).
[13]M. Y. Zhuravlev, S. S. Jaswal, and E. Y. Tsymbal, Appl. Phys. Lett. **87**, 222114 (2005).
[14]C. G. Duan, S. S. Jaswal, and E. Y. Tsymbal, Phys. Rev. Lett. **97**, 47201 (2006).
[15]S. Ju, T. Y. Cai, G. Y. Guo, and Z. Y. Li, Phys. Rev. B **75**, 064419 (2007).
[16]M. Gajek, M. Bibes, S. Fusil, K. Bouzehouane, J. Fontcuberta, A. Barthélémy, and A. Fert, Nature Mater. **6**, 296 (2007).
[17]S. Valencia, A. Crassous, L. Bocher, V. Garcia, X. Moya, R. O. Cherifi, C. Deranlot, K. Bouzehouane, S. Fusil, A. Zobelli, A. Gloter, N. D. Mathur, A. Gaupp, R. Abrudan, F. Radu, A. Barthélémy, and M. Bibes, Nature Mater. **10**, 753 (2011).
[18]D. Pantel, S. Goetze, D. Hesse, and M. Alexe, Nature Mater. **11**, 289 (2012).
[19]N. A. Hill, J. Phys. Chem. B **104**, 6694 (2000).
[20]J. P. Velev, C. G. Duan, K. D. Belashchenko, S. S. Jaswal, and E. Y. Tsymbal, J. Appl. Phys. **103**, 07A701 (2008).
[21]J. Junquera and P. Ghosez, Nature **422**, 506 (2003).
[22]D. D. Fong, G. B. Stephenson, S. K. Streiffer, J. A. Eastman, O. Auciello, P. H. Fuoss, and C. Thompson, Science **304**, 1650 (2004).
[23]M. Dawber, K. M. Rabe, and J. F. Scott, Rev. Mod. Phys. **77**, 1083 (2005).
[24]A. Petraru, H. Kohlstedt, U. Poppe, R. Waser, A. Solbach, U. Klemradt, J. Schubert, W. Zander, and N. A. Pertsev, Appl. Phys. Lett. **93**, 072902 (2008).
[25]M. Y. Zhuravlev, S. Maekawa, and E. Y. Tsymbal, Phys. Rev. B **81**, 104419 (2010).
[26]M. Q. Cai, Y. Zheng, P. W. Ma, and C. H. Woo, J. Appl. Phys. **109**, 024103 (2011).
[27]M. D. Glinchuk and A. N. Morozovska, J. Phys.: Condens. Matter **16**, 3517 (2004).
[28]A. M. Bratkovsky and A. P. Levanyuk, Phys. Rev. Lett. **94**, 107601 (2005).
[29]A. N. Morozovska, E. A. Eliseev, S. V. Svechnikov, A. D. Krutov, V. Y. Shur, A. Y. Borisevich, P. Maksymovych, and S. V. Kalinin, Phys. Rev. B **81**, 205308 (2010).
[30]S. Bin-Omran, I. Kornev, I. Ponomareva, and L. Bellaiche, Phys. Rev. B **81**, 094119 (2010).
[31]G. Kresse and J. Furthmüller, Phys. Rev. B **54**, 11169 (1996).
[32]See http://cms.mpi.univie.ac.at/vasp/ for VASP.
[33]A. M. Kolpak, N. Sai, and A. M. Rappe, Phys. Rev. B **74**, 054112 (2006).
[34]R. Resta, Ferroelectrics **136**, 51 (1992).
[35]D. Vanderbilt and R. D. King-Smith, Phys. Rev. B **48**, 4442 (1993).
[36]Y. Umeno, J. M. Albina, B. Meyer, and C. Elsässer, Phys. Rev. B **80**, 205122 (2009).
[37]See supplementary material at http://dx.doi.org/10.1063/1.4801306 for magnetic moments of interfacial atoms and side views of the relaxed structures of all MFTJs.